Energy Reports 8 (2022) 14888–14900

Contents lists available at ScienceDirect

Energy Reports

journal homepage: www.elsevier.com/locate/egyr

Research paper

Hybrid African vultures–grey wolf optimizer approach for electrical parameters extraction of solar panel models

Mahmoud A. Soliman [a], Hany M. Hasanien [b], Rania A. Turky [c], S.M. Muyeen [d,*]

[a] Electrical Engineering Department, Faculty of Engineering, Menoufia University, Shebin El-Kom 32511, Egypt
[b] Electrical Power and Machines Department, Faculty of Engineering, Ain-Shams University, Cairo 11517, Egypt
[c] Electrical Engineering Department, Faculty of Engineering and Technology, Future University in Egypt, Cairo 11835, Egypt
[d] Electrical Engineering Department, Faculty of Engineering, Qatar University, Doha, Qatar

ARTICLE INFO

Article history:
Received 24 May 2022
Received in revised form 11 October 2022
Accepted 24 October 2022
Available online 17 November 2022

Keywords:
Hybrid African vultures–grey wolf optimizer approach
Photovoltaic modeling
PV parameters extraction
Solar energy
Three-diode model

ABSTRACT

Three-diode model (TDM) of photovoltaic (PV) cells is a significantly precise model that addresses the electrical and optical losses in such PVs. Due to its nonlinearity and multivariable characteristics, the TDM is a complex and debatable PV model. This article proposes a novel hybrid African vultures–grey wolf optimizer (AV–GWO) approach to precisely estimate the electrical parameters of such TDM. The AVO is a novel meta-heuristic approach inspired by African vultures' behavior in nature. In the hybrid approach offered, the vultures' updating position formula of the AVO is applied to update the key-group parameters in GWO, resulting in an enhanced GWO approach. A new objective function that depends on the current error is proposed in this study, which the AV–GWO minimizes to precisely estimate the optimal nine parameters of such TDM. The nine electrical parameters attained through the hybrid AV–GWO approach are compared with that obtained via other meta-heuristic methods. In that regard, the AV–GWO approach has achieved superior and outstanding outcomes. For more realistic studies, the offered AV–GWO is efficiently utilized to design the optimal parameters of TDM for two industrial KC200GT and MSX-60 PV cells. In the optimization process, the hybrid AV–GWO has recorded the lowest optimal fitness values of 8.475e−13 and 7.412e−12 for KC200GT and MSX-60, respectively. Additionally, the AV–GWO has recorded the shortest computing time in 0.43412 (s) and 0.3142 (s) for KC200GT and MSX-60, respectively, which reflects its rapid convergence, supremacy, and stability, among other approaches. Those PV cells' modeled *I-V* and *P-V* curves closely coincide with the real data measured under various climatic conditions. The error between these results is less than 0.4%. The high performance of the hybrid AV–GWO approach-based TDM is verified by examining its absolute current error with that realized from other PV models. Consequently, the outcomes have depicted that the offered AV–GWO approach is superior and can be used to generate a precise PV model of any industrial PV cell, which is a unique addition to the PVs market.

1. Introduction

Over recent decades, the development of sustainable and renewable energy sources (RESs) has been on rapid embarkation around the globe because of several serious factors, including fossil energy consumption, the rise in fuel prices, political issues, and considerable concerns about achieving a healthy atmosphere (Zhang et al., 2020a; Ridha et al., 2020; Qais et al., 2019). Among various RESs, solar photovoltaic (PV) energy is the most popular technology widely installed worldwide. Newly, the PV sector has seen significant economic growth due to the cost decrease in PV components and power converters, enhancing the competitiveness and efficiency of this PV technology more than other RESs. This indicates the numerous endeavors exerted in developing the PV industry. Based on the global PV market statistics, 142 GW of global PV installed capacity was achieved at the end of 2020, which indicates a 14% growth compared to 2019's record. It is predicted that 2.8 TW of global PV installations will be attained by 2030 (PV Power Plants, 2020). The reported records denote the massive integration of solar PV installations into power grids. Accordingly, grid-integrated PV power plants can release several problems. To address the efficacy of PV systems on the power grids under different environmental situations and examine the effect of transient grid disturbances on the PV power systems through simulation studies, accurate modeling of such PVs is significantly desired.

* Corresponding author.
E-mail addresses: dr.msoliman08@gmail.com (M.A. Soliman), hanyhasanien@ieee.org (H.M. Hasanien), rania.turky@fue.edu.eg (R.A. Turky), sm.muyeen@qu.edu.qa (S.M. Muyeen).

https://doi.org/10.1016/j.egyr.2022.10.401

The mathematical modeling of such PV cells is expressed via nonlinear *I-V* behavior, which includes numerous unknown electrical parameters owing to the insufficient data the manufacturers supplied (Sharma et al., 2021a). In the PV modules, two types of losses are presented, *i.e*., electrical and optical losses (El-Fergany, 2021; Kassis and Saad, 2010). Electrical losses are defined as: (*i*) conduction losses in the wires and soldered junction that can be simulated by a series resistance (R_s), and (*ii*) leakage current inside the PV cells that is simulated by a parallel resistance (R_p). On the other hand, optical losses inside the PV cell are caused by diffusion in the quasi-neutral zone, recombination in the depletion layer, and recombination at the grain boundaries (Ma et al., 2021).

The PV modeling should appear all the PV losses. The ideal PVs are represented by a photo-generated current (I_{PV}) which is pertinent to the amount of solar irradiation that drops on them. The real I_{PV} is different owing to the electric and visual losses in the P-N junction of such PVs, resulting in a single-diode model (SDM) (El-Fergany, 2021). This model is characterized by its simple design and fast dynamic behavior. The SDM can represent the diffusion and recombination losses in the quasi-neutral region of the emitter and majority zones in the P-N junction. To attain precise PV modeling, a two-diode model (DDM) is introduced to address the PV losses in the quasi-neutral and space-charge of the P-N junction and the SDM losses. Recently, the three-diode model (TDM) appeared to address the recombination in defect regions and grain boundaries and the losses in the SDM and DDM. Therefore, TDM can represent all losses in three areas of the P-N junction of such PV cells. Hence, TDM is considered a more accurate PV modeling of such PV modules (Elazab et al., 2018) considered in this study. The TDM of such PVs involves several parameters like photo-generated current (I_{PV}), series resistance (R_s), parallel resistance (R_p), emission coefficient of three diodes (a_1, a_2, a_3), and leakage current for three diodes (I_{o1}, I_{o2}, I_{o3}) (Qais et al., 2019). Hence, it is crucial to find those parameters to obtain a proper PV model critical in simulation assessments of grid-integrated PV systems.

Several strategies were used to define the electrical parameter of various PV panels accurately. In the PV literature, SDM and DDM of PV panels are extensively examined because of their limited number of unknowns that can be estimated using analytical approaches, iterative approaches, and various optimizer algorithms. Analytical methods are employed for extracting the unknowns using several vital factors, which are available in the PV datasheet, including short-circuit current (I_{SC}), open-circuit voltage (V_{OC}), and maximum power (P_m). These methods are distinguished by their fast convergence and the absence of any measurements. However, some derivations are applied to limit the undetermined parameters, including ignoring R_p (Khanna et al., 2015), primary values of such resistance (Di Piazza et al., 2017) and I_o (Şenturk, 2018), a Lambert technique (Polo et al., 2019), and utilizing the least square error method (Toledo et al., 2018). The analytical techniques require different assumptions and several differentiations of dynamic equations, leading to unrealistic solutions. To estimate the unknowns, the analytical and optimizer methods are integrated to precisely design the DDM parameters (Chennoufi et al., 2021; Bradaschia et al., 2019b). Several iterative techniques are utilized to fine-tune the PV parameters, like the Gauss–Seidel method (Chatterjee et al., 2011) and Newton–Raphson (Ridha et al., 2021). These approaches are hampered by solid nonlinearity and multi-variability, which lack precision (El-Fergany, 2021; Elazab et al., 2018). Moreover, the accuracy of analytical and iterative methods is limited since the primary solutions are not always optimal. Besides, they need good initial values to avoid divergence.

To overcome the nonlinearity and complexity of such methods, meta-heuristic approaches based on artificial intelligence optimization algorithms are effectively utilized to precisely design the electrical parameters of the PV modules. Genetic algorithm (GA) (Bastidas-Rodriguez et al., 2017), Nelder–Mead moth flame algorithm (Zhang et al., 2020a), whale optimization algorithm (WOA) (Elazab et al., 2018), boosted mutation-based Harris hawks optimizer (Ridha et al., 2020), artificial ecosystem-based optimization (Yousri et al., 2020a), stochastic fractal search optimization algorithm (Rezk et al., 2021), chaotic whale optimization algorithm (Oliva et al., 2017), Random learning gradient-based optimization (Zhou et al., 2021), Laplacian Nelder–Mead spherical evolution (Weng et al., 2021), improved wind-driven optimizer (Ibrahim et al., 2020), Emended heap-based optimizer, (Rizk-Allah and El-Fergany, 2021). Other heuristic algorithms (Sharma et al., 2021b; Ramadan et al., 2021; Bradaschia et al., 2019a; Zhang et al., 2020b; Li et al., 2019; JackChin and Salam, 2019; Marques Gomes et al., 2017) are utilized for identifying the undetermined parameters of such PV models by optimizing the fitness functions. Different fitness function-based datasheets have been presented and employed different optimizer algorithms to address these problems, like the bacterial foraging method (Awadallah and Venkatesh, 2016), differential evolution approaches (Gao et al., 2018; Patro and Saini, 2020), and artificial bee colony optimizer algorithm (Oliva et al., 2014). Because of the range selection of upper and lower parameter limits, such as the dark saturation current that is extremely sensitive, these approaches are ineffective.

Nowadays, a TDM has been applied to achieve an accurate PV modeling that addresses all the PV losses. This model involves nine parameters that are needed to be identified to attain a precise PV model. However, because of the multivariable and low number of nonlinear equations, it is hard to identify the nine parameters of this TDM using analytical approaches. The optimization approaches play an essential role in designing the unknown parameters by minimizing the objective function. Different optimizer approaches are developed to correctly create the nine parameters of such TDM like a sunflower optimizer algorithm (SOA) (Qais et al., 2019), WOA (Elazab et al., 2018), Laplacian Nelder–Mead spherical evolution (Weng et al., 2021), improved wind-driven optimizer (Ibrahim et al., 2020), Emended heap-based optimizer (Rizk-Allah and El-Fergany, 2021), tree growth-based optimizer algorithm (Diab et al., 2020), advanced particle swarm optimizer (Yousri et al., 2020b), and manta ray optimization algorithm (Houssein et al., 2021). Notably, these approaches cannot provide assurance for the achievement of the global solution. Still, an effort is being made on this subject to raise the probability of avoiding being locked into local minima by inventing new algorithms. In this regard, there is still potential for development. The Meta-heuristic approaches are the most promising solutions to solve different engineering problems; each has advantages and disadvantages. No one method can solve all engineering optimization issues due to the difference in the degree of nonlinearity, convexity, separability of the control variables, and modality.

As per the no-free lunch principle, one approach cannot adequately get the optimal solution to these difficulties, which impute the researchers to employ several hybrid optimization algorithms to detect enhanced solutions and eventually extract the TDM parameters. Furthermore, the search spaces of these algorithms are purposefully constrained to avoid stagnation in a local solution. As a result, the fundamental purpose of this research is to create a simple, fast converging, and stable hybrid algorithm that can be used for a wide range of search spaces.

Many hybrid algorithms are presented to precisely identify the electrical parameters of TDM-based PV modules like improved slime mould optimizer and Lambert W-function (El-Fergany, 2021), hybrid marine predators-slime mould algorithm (Yousri et al.,

2021), hybrid adaptive teaching optimization and differential evolution (Li et al., 2020), and analytical approaches and optimizer algorithms are combined to estimate the PV parameters (Qais et al., 2019) correctly.

This study introduces a novel hybrid African vultures-grey wolf optimizer (AV–GWO) approach to extract the nine parameters of such TDM. The AVO algorithm represents a new nature meta-heuristic approach, presented in 2021 by Abdollahzadeh et al. (2021). It was inspired by the natural activity of African vultures (Abdollahzadeh et al., 2021). The AVO is a robust nature optimizer algorithm with various features, including a minimum number of variables to design, a simple method, low computation burden, quick convergence speed, flexibility, and a gradient-free nature. Hence, the AVO can be appointed to solve various difficulties in power systems effectively. The AVO approach was evaluated on 36 standard benchmark functions, and it was employed to find optimal solutions for eleven engineering problems, which indicates the significant superiority of such AVO. In the hybrid approach, the vultures' updating position formula of the AVO is applied to update the key-group parameters in GWO, resulting in an enhanced GWO approach.

This article proposes a novel hybrid AV–GWO approach to precisely estimate the electrical parameters of such TDM. A new objective function that depends on the current error is presented in this study, which is minimized by the hybrid AV–GWO to precisely estimate the optimal nine parameters of such TDM. The nine electrical parameters attained through the hybrid AV–GWO approach are compared with that obtained via other meta-heuristic methods. In that regard, the AV–GWO approach has achieved superior and outstanding outcomes. For more realistic studies, the offered AV–GWO is efficiently utilized to design the optimal parameters of TDM for two industrial KC200GT and MSX-60 PV cells. In the optimization process, the hybrid AV–GWO has recorded the lowest optimal fitness values of 8.475e−13 and 7.412e−12 for KC200GT and MSX-60, respectively. Additionally, the AV–GWO has recorded the shortest computing time in 0.33412 (s), which reflects its rapid convergence, supremacy, and stability among other approaches. Those PV cells' modeled I-V and P-V curves closely coincide with the real data measured under various climatic conditions. The error between these results is less than 0.4%. The high performance of the hybrid AV–GWO approach-based TDM is verified by examining its absolute current error with that realized from other PV models. Consequently, the outcomes have depicted that the offered AV–GWO approach is superior and can be used to generate a precise PV model of any industrial PV cell, which is a unique addition to the PVs market.

The following statements illustrate the main novelty of this paper:

- Introducing the hybrid African vultures–grey wolf optimizer (AV–GWO) approach.
- A new objective function that depends on the current error is proposed in this study.
- AV–GWO, AVO, GWO, WOA, and other meta-heuristic algorithms are applied to find the optimal nine parameters of TDM for two distinct marketable PV cells.
- Comparing the statistical analyses of 30 separate runs of all algorithms, where the offered AV–GWO algorithm has achieved the shortest computing time and lowest optimal fitness value of the marketable PV cells.
- The modeled *I-V* and *P-V* curves of the distinct PV cells are compared with the real measured data under various climatic conditions using the hybrid AV–GWO algorithm.
- The absolute current error of the hybrid AV-GWO-based TDM is compared with that realized using other approaches-based PV models.

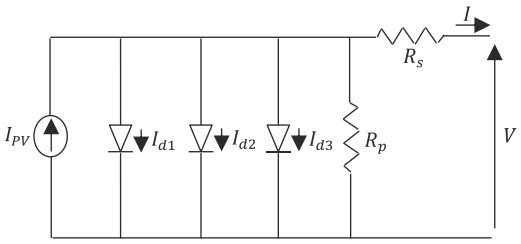

Fig. 1. TDM of PV panel.

The remainder of this article is prepared as follows; Section 2 describes the TDM of the PV module. In Section 3, the problem formulation is proposed. The AVO technology is presented in Section 4. The GWO overview is illustrated in Section 5. Section 6 describes the detailed hybrid AV–GWO approach. Section 7 depicts the simulation analyses and discussion. Section 8 draws conclusions and recommendations for further work.

2. Three-diode model of PV module

Various equivalent circuits are employed to represent the nonlinear *I-V* relationship of SDM, DDM, and TDM of such PV panels. Fig. 1 indicates the equivalent electrical circuit of the TDM of PV modules, which includes a photo-current source, three parallel diodes, and series and parallel resistors (Qais et al., 2019). The mathematical *I-V* behavior of TDM of PV modules is described using the following equation (Ramadan et al., 2021; Qais et al., 2019):

$$\begin{aligned} I = I_{PV} &- I_{O1}\left\{exp\left[\frac{V+IR_s}{a_1\ V_t}\right]-1\right\} \\ &- I_{O2}\left\{exp\left[\frac{V+IR_s}{a_2\ V_t}\right]-1\right\} \\ &- I_{O3}\left\{exp\left[\frac{V+IR_s}{a_3\ V_t}\right]-1\right\} - \frac{V+IR_s}{R_p} \end{aligned} \tag{1}$$

where $V_t = N_s KT/q$, N_s depicts the number of series connected cells, K indicates the Boltzmann constant, T is panel surface temperature, and q represents the electron charge.

In the PV datasheet, there are many noticeable points of the *I-V* relationship, including I_{SC}, $V_{OC,}$ and P_m. Various formulas are set to demonstrate the characteristics of PV panels at several temperatures and solar irradiances, as follows (De Soto et al., 2006; Sera et al., 2007):

$$I_{PV} = \left(I_{PV,n} + K_I \Delta T\right)\frac{G}{G_n} \tag{2}$$

$$I_O = I_{On}\left(\frac{T}{T_n}\right)^3 e^{\left\{\frac{qE_g}{aK}\left[\frac{1}{T_n}-\frac{1}{T}\right]\right\}} \tag{3}$$

$$E_g = E_{g,n}(1 - 0.0002677)\Delta T \tag{4}$$

$$R_p = R_{P,n}\frac{G}{G_n} \tag{5}$$

where the variable subscript by n is the variable obtained under standard test conditions (STC). K_I indicates the short circuit current–temperature coefficient, ΔT stands for temperature difference, G is actual irradiance, and E_g denotes band gap characteristic. $E_{g,n}$ is considered to be 1.211 eV (Elazab et al., 2018; Qais et al., 2019). Huge efforts are exerted to identify the unknowns of the PV panel. Here, the nine parameters of the TDM that needed to determine are (I_{PV}, I_{O1}, I_{O2}, I_{O3}, R_s, R_p, a_1, a_2, *and* a_3).

3. Problem formulation

In this paper, various optimizer algorithms are employed to determine the TDM's parameters of the PV module, which require a definition of a fitness function. A new fitness function is presented here to design the TDM precisely. The current error, defined as the change between the estimated and measured model currents, is utilized as the fitness function in the optimization approach. The offered fitness function is the sum of three terms, which are the absolute current error, the squared current error, and the current error to the power of four, and can e represented as follows:

$$\varepsilon = \sum_{k=1}^{N} |f_k(V, I, \phi)| + \sum_{k=1}^{N} f_k^2(V, I, \phi) + \sum_{k=1}^{N} f_k^4(V, I, \phi) \tag{6}$$

where N refers to the measured data samples, ϕ is a vector that represents the design variables of the TDM parameters, and precisely needed to be computed. The $f_k(V, I, \phi)$ is mathematically formulated using (7):

$$f_k(V, I, \phi) = I_{PV} - I_{O1}\left\{exp\left[\frac{V + IR_s}{a_1 V_t}\right] - 1\right\} - I_{O2}\left\{exp\left[\frac{V + IR_s}{a_2 V_t}\right] - 1\right\} - I_{O3}\left\{exp\left[\frac{V + IR_s}{a_3 V_t}\right] - 1\right\} - \frac{V + IR_s}{R_p} - I_{measured} \tag{7}$$

where $\phi = \{I_{PV}, I_{O1}, I_{O2}, I_{O3}, R_s, R_p, a_1, a_2, a_3\}$.

$I_{measured}$ refers to the measured current from the PV module. Then, the hybrid AV–GWO approach is applied to minimize the objective function, ε, and extract the TDM parameters. The principle AV–GWO code is created using MATLAB environment (Release, 2016b).

4. African vultures–grey wolf optimizer overview

Meta-heuristic optimization algorithms play a vital role in various applications' optimization and engineering problems. Such approaches are motivated by foraging creatures and animals in nature. The AVO algorithm simulates the behavior and foraging of vultures in nature in terms of obtaining food and feeding multiple vultures in Africa (Abdollahzadeh et al., 2021). The AVO is a new nature meta-heuristic approach, modeled in 2021 by Abdollahzadeh et al. (2021). In Africa, various types of vultures live, and each has some lifestyle behaviors in fighting and finding food. Vultures are constantly traveling great distances in quest of food. In this travel, vultures move in a rotational flight to find food. Vultures become aggressive when they are starving. The AVO approach was evaluated on 36 standard benchmark functions and was employed to find optimal solutions for eleven engineering problems (Abdollahzadeh et al., 2021).

4.1. African vultures optimization process

Vultures are classified into two groups in nature, and each has a different insufficiency in finding food. The vultures have been searching for food, prompting them to flee the hungry trap. At first, it was considered that the worst solution is the weakest, and vultures tend to avoid the worst. AVO considers two of the best solutions to be the strongest and best vultures, while others try to get close to them. The AVO algorithm is formulated in four steps, as follows.

Phase 1: *Choosing the best vulture from any group*

The populations are initially randomized in the search space. The fitness values of these agents are computed, where the best agent in the first group is picked as the first-best solution, and the best agent in the second group is chosen as the second-best solution. The rest solutions are moved to the first and second groups by utilizing (8). The whole population is recalculated in each iteration (Abdollahzadeh et al., 2021).

$$R(i) = \begin{cases} Best\ vulture_1 & if\ p_i = L_1 \\ Best\ vulture_2 & if\ p_i = L_2 \end{cases} \tag{8}$$

where L_1 and L_2 represent the probability parameter (p_i) that is utilized to select the first-best vulture and the second-best vulture, respectively. Besides, these parameters determine the probability of moving other agents to one of the best solutions and their values between [0, 1]. This process is performed using the Roulette wheel mechanism, as in the following formula.

$$p_i = \frac{F_i}{\sum_{i=1}^{n} F_i} \tag{9}$$

where F stands for the vultures' starvation rate.

Phase 2: *The vultures' starvation rate*

African vultures are constantly looking for food and have tremendous energy when overstuffed, making them fly far away searching for food. When vultures are starving, they lack the energy to fly and search for food. Besides, they become more aggressive. This behavior can be mathematically simulated using (10) (Abdollahzadeh et al., 2021).

$$t = h \times \left(sin^w\left(\frac{\pi}{2} \times \frac{iter_i}{iter_{max-i}}\right) + \left(cos^w \frac{\pi}{2} \times \frac{iter_i}{iter_{max-i}}\right) - 1\right) \tag{10}$$

$$F = (2 \times rand_1 + 1) \times z \times \left(1 - \frac{iter_i}{iter_{max-i}}\right) + t \tag{11}$$

where F stands for the vultures are overstuffed, $iter$ denotes the current iteration, $iter_{max}$ denotes the number of iterations, and z stands for randomizing number $[-1, 1]$ that changes in each iteration. h denotes randomizing number $[-2, 2]$. $rand_1$ denotes a random value [0, 1]. If the z value falls under zero, the vultures will be hungry, and when this value increases to zero, the vultures are overstuffed.

Eq. (10) has been employed to escape from local optimal points. In the AVO algorithm, the exploitation step is carried out at the algorithm's final iterations, and the exploration phase is also done in some final iterations of such an AVO. The main goal of this strategy is to modify (10) to vary the exploration and exploitation phases to raise the possibility of eventually joining the exploratory phase throughout the AVO optimization process. In (10), w is a fixed parameter affecting the algorithm processes. When the value of $|F|$ is > 1, vultures look for food in various locations, and the AVO algorithm begins the exploration phase. If $|F|$ is < 1, the AVO algorithm reaches the exploitation phase, and vultures are looking for food near the solutions.

Phase 3: *Exploration*

The AVO algorithm's exploration phase is explained in this step. Vultures have the visual ability to find sick animals. Vultures spend a long time examining their surroundings and flying vast distances in quest of food. Vultures in the AVO can check numerous random regions by using two techniques, and a parameter P_1 is utilized to choose one of them. This parameter is set before

the search procedure, and its value ranges [0, 1]. Each vulture searches for satiation in the surroundings at random.

$$P(i+1) = \begin{cases} \text{Eq. (13)} & \text{if } P_1 \geq rand_{P1} \\ \text{Eq. (14)} & \text{if } P_1 < rand_{P1} \end{cases} \quad (12)$$

$$P(i+1) = R(i) - D(i) \times F \quad (13)$$

$$D(i) = |X \times R(i) - P(i)| \quad (14)$$

where $R(i)$ denotes one of the best vultures selected and P_i is the vulture position vector. X is a vector coefficient that refers to the vultures' unpredictable movement to defend food from other vultures, which varies with each iteration and can be achieved using $X = 2 \times rand$. $P(i+1)$ denotes the vulture location in the next iteration.

$$P(i+1) = R(i) - F + rand_2 \times ((ub - lb) \times rand_3 + lb) \quad (15)$$

where $rand_2$ is a random value between [0, 1]. ub and lb are the upper and lower limits of the variables. $rand_3$ is utilized to raise the coefficient of a random nature. This enhances the variety and number of searches in various search space areas.

Phase 4: *Exploitation*

This stage examines the efficiency of the AVO algorithm. If the value of $|F|$ is < 1, the AVO begins the exploitation phase, divided into two phases with distinct tactics. P_2 and P_3 indicate the parameters utilized to choose the strategies available in the first phase and the second phase, respectively, and their values between [0, 1].

In the AVO, the exploitation phase occurs when the value $|F|$ is between [1, 0.5], in which the rotating flight and siege-fight techniques are performed. P_2 is valued before the searching operation to determine whether each strategy is selected. In this phase, $rand_{P2}$, which denotes a random number between [0,1], is produced. If $rand_{P2} \geq P_2$, the Siege-fight strategy is performed. While, if $rand_{P2} < P_2$, the rotating flight strategy is implemented as follows.

$$P(i+1) = \begin{cases} \text{Eq. (17)} & \text{if } P_2 \geq rand_{P2} \\ \text{Eq. (20)} & \text{if } P_2 < rand_{P2} \end{cases} \quad (16)$$

Food Competitively: When $|F| \geq 0.5$, the vultures are overstuffed and are high-powered. When many vultures get together in one food, it can lead to significant conflicts over food acquisition. At some times, vultures do not share food with others. The weaker vultures try to eat from the healthy ones by gathering around them. This can cause minor conflicts. The following equations model this step.

$$P(i+1) = D(i) \times (F \times rand_4) - d(t) \quad (17)$$

$$d(t) = R(i) - P(i) \quad (18)$$

where F denotes the satiation rate of vultures, $rand_4$ refers to a random number between [0, 1], which is utilized to raise the random coefficient.

Vultures flying in a circle: Vultures are used to fly in a rotational flight. Spiral motion has been used to express this flight, which is established between all vultures and one of the two best vultures. This stage can be mathematically illustrated as follows:

$$S_1 = R(i) \times \left(\frac{rand_5 \times P(i)}{2\pi}\right) \times \cos(P(i)) \quad (19)$$

$$S_2 = R(i) \times \left(\frac{rand_6 \times P(i)}{2\pi}\right) \times \sin(P(i)) \quad (20)$$

$$P(i+1) = R(i) - (S_1 + S_2) \quad (21)$$

From the previous Eqs., $R(i)$ denotes the location vector of one of the two best vultures in the existing iteration, which is realized using (8), $rand_5$ and $rand_6$ are random numbers between [0, 1]. The vultures location is updated using (21).

Second Phase: *Exploitation*

In the 2nd phase of exploitation, The actions of the two vultures attract many kinds of vultures to the feeding source and the aggressive life to obtain food. If $|F| < 0.5$, this phase is accomplished. In this phase, $rand_{P3}$ is generated. If $rand_{P3} \geq P_3$, the plan is to gather a variety of vultures around the food supply. The aggressive fight strategy is performed if the generated value is $<$ P3.

$$P(i+1) = \begin{cases} \text{Eq. (25)} & \text{if } P_3 \geq rand_{P3} \\ \text{Eq. (26)} & \text{if } P_3 < rand_{P3} \end{cases} \quad (22)$$

Vultures' gathering over the food source: The vultures' movement toward the food source is checked. When several vultures are hungry, they may get together in one food source. This movement can be formulated as follows:

$$A_1 = Best\ Vulture_1(i) - \frac{Best\ Vulture_1(i) \times P(i)}{Best\ Vulture_1(i) \times P(i)^2} \times F \quad (23)$$

$$A_2 = Best\ Vulture_2(i) - \frac{Best\ Vulture_2(i) \times P(i)}{Best\ Vulture_2(i) \times P(i)^2} \times F \quad (24)$$

where $Best\ vulture_1(i)$ and $Best\ vulture_2(i)$ are the best vultures of the first and second groups, respectively, in the current iteration.

$$P(i+1) = \frac{A_1 + A_2}{2} \quad (25)$$

Finally, the gathering of vultures is performed using (25). $P(i+1)$ denotes the vector of the vulture's location in the next iteration. *Aggressive Competition for Food:* When $|F| < 0.5$, the head vultures are frail and hungry, and they lack the strength to deal with other vultures. The other vultures become aggressive in their search for food. Besides, they travel in different ways toward the vultures' heads. This motion is modeled as follows:

$$P(i+1) = R(i) - |d(t)| \times F \times Levy(d) \quad (26)$$

where $d(t)$ denotes the distance of the vulture to one of the best vultures of the two groups, which is obtained using (18). Levy flight (LF) styles are employed to raise the efficiency of the AVO and can be obtained using the following equation:

$$LF(x) = 0.01 \times \frac{u \times \sigma}{|v|^{\frac{1}{\beta}}}\sigma = \left(\frac{\tau(1+\beta) \times \sin\left(\frac{\pi\beta}{2}\right)}{\tau\left(1+\beta^2\right) \times \beta \times 2\left(\frac{\beta-1}{2}\right)}\right)^{\frac{1}{\beta}} \quad (27)$$

where d denotes the problem dimensions, u and v stand for a random number varying between [0, 1], $\sigma > 0$ denotes the standard deviation, and β is a fixed number of 1.5.

The computational complexity of the AVO approach is based on the initialization process, fitness assessment, and updating of vultures. The computational intricacy in the updating process is determined by looking for the optimal position. The AVO approach begins with a random population of solutions, which is enhanced till the process is terminated. The pseudo-code and the flowchart of the AVO approach are depicted in Figs. 2 and 3, respectively.

5. Grey wolf optimizer overview

GWO is a meta-heuristic-based swarm intelligence approach motivated by the grey wolf hunting procedure in nature. The GWO was introduced by Mirjalili et al. in 2014. Grey wolves tend to congregate in groups. On average, each group has 5–12 members, which is divided into four dominating individuals;

Start the population Size N and $Iter_{max}$
Outputs: The location of Vulture and its fitness value
Initialize the random population $\boldsymbol{P_i}$ *(i=1,2,……N)*
while *(stopping condition is not met)* ***do***
  Calculate the fitness values of Vulture
  Set $\boldsymbol{P_{Best\ Vulture1}}$ *as the location of Vulture (1st best location Best Vulture Category 1)*
  Set $\boldsymbol{P_{Best\ Vulture2}}$ *as the location of Vulture (2nd best location Best Vulture Category 2)*
  For *(each Vulture (*$\boldsymbol{P_i}$*))* ***do***
  Select $R(i)$ using (8)
  Update F using (11)
  if ($|F| \geq 1$) **then**
    if ($P_1 \geq rand_{P1}$) **then**
      Update the vulture's location using (13)
    else
      Update the vulture's location using (15)
    if ($|F| < 1$) **then**
      if ($|F| \geq 0.5$) **then**
        if ($P_2 \geq rand_{P2}$) **then**
          Update the vulture's location using (17)
        else
          Update the vulture's location using (21)
      else
        if ($P_3 \geq rand_{P3}$) **then**
          Update the vulture's location using (25)
        else
          Update the vulture's location using (26)
Return $\boldsymbol{P}_{Best\ vulture\ 1}$

Fig. 2. Pseudo-code of the AVO approach.

alpha (α), beta (β), delta (δ), and omega (ω) wolves (Mirjalili et al., 2014).

In each group, the pack's leaders and most dominating are α wolves. They make the decisions about hunting, sleeping, and when to wake up. Besides, α wolves follow other wolves in the pack to achieve democratic behavior. The α wolf is not the most powerful member of the group, but they are effective in controlling and arranging the group. The second most dominant members in the group are β wolves. They assist α wolves in making choices and other pack operations. When the α wolves die or get too old, the β wolves are the best choices. The primary function of β wolves is to counsel the α wolves and control the group. The ω wolves are the group's lowest level, where they are the last wolves that are allowed to eat. In certain circumstances, the ω wolves serve as the pack's babysitters. The δ wolves are in charge of sending data to α and β wolves. They also control ω wolves. This category includes scouts, elders, hunters, sentinels, and caregivers. The critical stages of grey wolf hunting are as follows (Mirjalili et al., 2014):-

1- Following, pursuing, and approaching the target.
2- Encircling and pestering the prey until it comes to a halt.
3- Launch an attack on the prey.

The GWO algorithm is mathematically simulated as follows:-

a. Social Hierarchy

The wolves' social hierarchy is simulated by assuming the α wolf to be the first fittest solution. The second and the third fittest solution are β and δ wolves, respectively. The only remaining option is regarded as the ω wolves. The optimization process, in general, is guided by α, β, and δ wolves. These wolves are tracked by ω wolves.

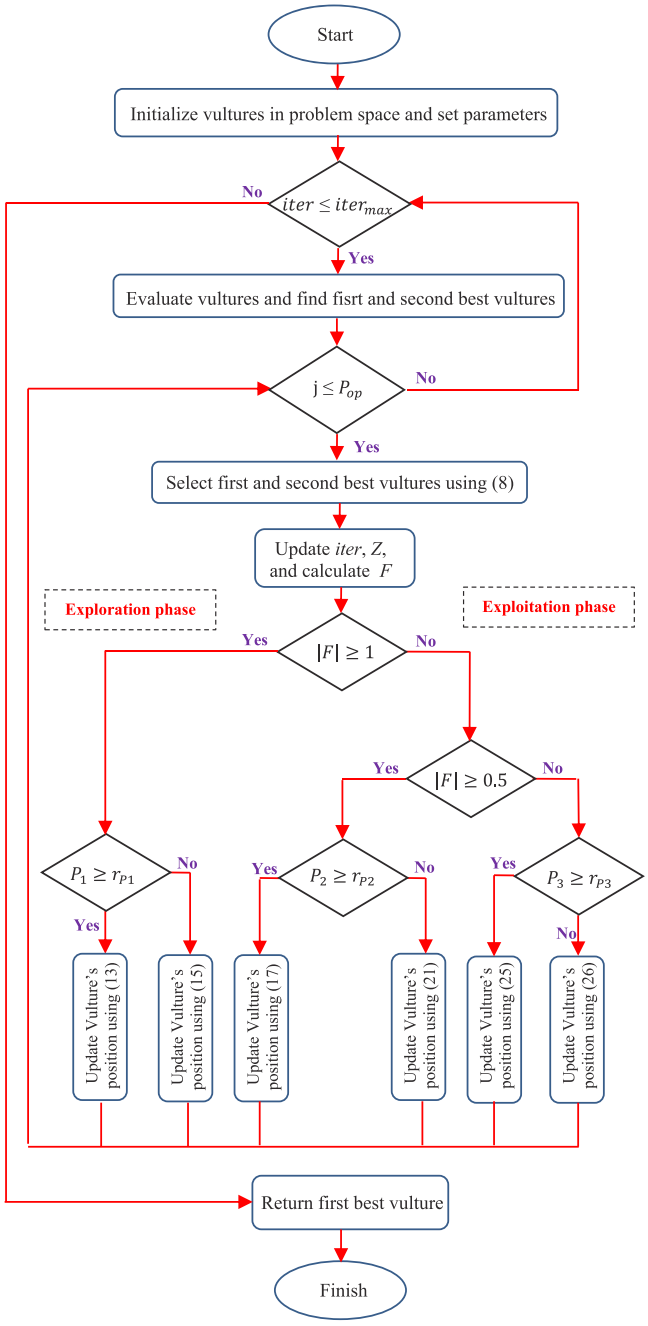

Fig. 3. Flowchart of the AVO-Approach.

b. Encircling the Prey

During the hunt, the grey wolves surround the victim. This process is mathematically simulated as follows:

$$D = |C.X_P(t) - X(t)| \tag{28}$$

$$X(t+1) = X_P(t) - A.D \tag{29}$$

where D indicates the dimension of a problem, A and C denote coefficient vectors, t refers to the current iteration, $X(t)$ and $X_P(t)$ point out the position vector of the grey wolf and the prey, respectively. The A and C vectors are determined as follows:

$$A = 2a.r_1 - a \tag{30}$$

$$C = 2.r_2 \tag{31}$$

During iterations, the components of vector a have linearly decreased from 2 to 0. r_1 and r_2 are random vectors between [0, 1].

c. Hunting

The grey wolf hunting strategy is modeled by assuming the α (best candidate solution), β, and δ wolves have enough knowledge about the prey's position. So, the top three best solutions produced so far are preserved and used to persuade additional search agents (including ω) to update their positions according to the best search agents' location. This hunting process is mathematically simulated as follows:

$$D_\alpha = |C_1.X_\alpha - X|, D_\beta = \left|C_2.X_\beta - X\right| D_\delta = |C_3.X_\delta - X| \tag{32}$$

$$X_1 = X_\alpha - A_1.D_\alpha, X_2 = X_\beta - A_2.D_\beta, X_3 = X_\delta - A_3.D_\delta \tag{33}$$

$$X(t+1) = \frac{X_1 + X_2 + X_3}{3} \tag{34}$$

d. Attacking the Prey

The grey wolf closes its hunt by attacking the prey after it stops moving. The attacking process is mathematically simulated by decreasing the value of vector a from 2 to 0 during the iterations. It has been noticed that $|A| < 1$ forces the wolves to assault the prey. The attacking methodology indicates the exploitation of the GWO algorithm.

e. Searching for the prey

The grey wolves typically go out in search of prey, according to the position of α, β, and δ wolves. The wolves begin by splitting from each other, searching for the prey, and then converging to assault the prey. It is noticed that $|A| > 1$ causes the wolves to seek out more fit prey. This divergence strategy depicts the GWO algorithm's exploration. The GWO flowchart is depicted in Fig. 4. The GWO approach begins with a random population of grey wolves and works its way up to the best candidate solution (X_α). The GWO was successfully applied to solving various optimization issues, as mentioned in El-Fergany and Hasanien (2015) and Soliman et al. (2018). The GWO has some merits, including simple to perform, a free-derivative algorithm, fewer operators to fine-tune, and it can save information about the search space via iterations and saves the best-obtained solution.

6. Hybrid african vultures–grey wolf optimizer overview

At present, the hybridization of two or more algorithms has become famous for detecting enhanced solutions to optimization problems. Several sets of well-known optimization approaches have been integrated into hybrid algorithms to become more effective in dealing with practical challenges.

When GWO explores an individual with a good fitness value, poor global search ability happens, making it possible to fall into the local optima. AVO algorithm updates the vultures' location with a given probability independent of the search path and in random directions. Therefore, moving from one region to another in AVO is more straightforward. As a result, AVO is a beneficial technique for GWO enhancement. This signifies that AVO is employed to update the location's current search agent and get a new set. Fig. 5 indicates the flowchart of the integrated AV–GWO approach.

As previously indicated, one of the most current integrations of optimization algorithms is the AVO with the GWO, where the AVO is applied to update the key-group parameters in GWO, as illustrated in the flow chart. The novel hybrid AV–GWO approach provides efficient solutions to optimization challenges.

In that regard, to modify the locations, convergence precisions, and speeds of the grey wolf agent (α), the position-updated formula of the AVO is applied to strike a balance between re-searching, exploiting, and expanding the convergence attitude of the GWO approach. Consider the GWO algorithm's remaining procedure as it is.

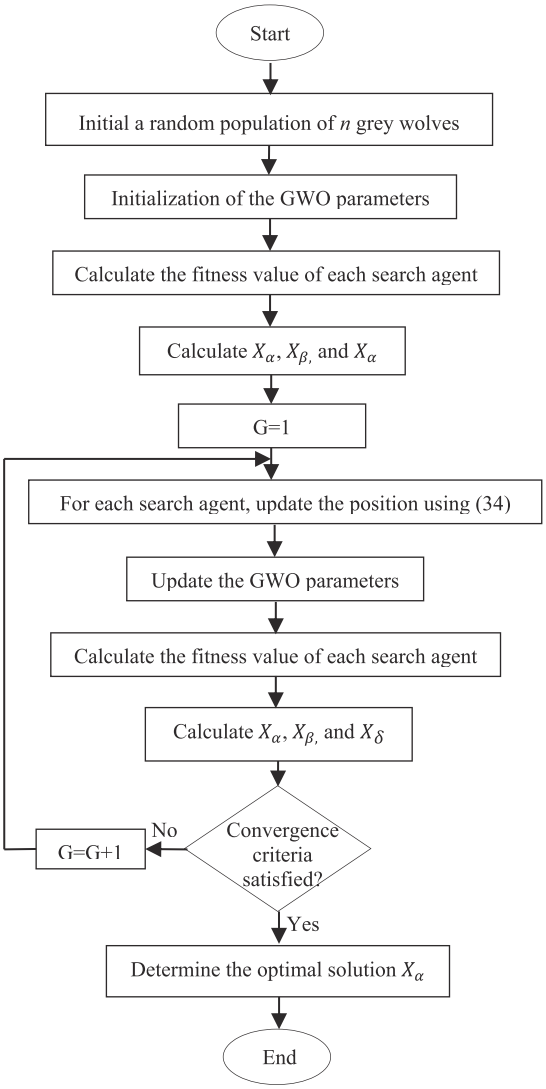

Fig. 4. Flowchart of The GWO approach.

7. Simulation analyses and discussion

This section exhibits the optimization and simulation outcomes for the TDM of PV cells using the hybrid AV–GWO approach. These approaches are presented to design the nine electrical parameters of the TDM of two practical PV panels, *i.e.*, Kyocera KC200GT (Kyocera, 2018) and Solarex MSX-60 (Solarex, 2018) PV panels. These panels utilized different cell types (Multicrystalline or Polycrystalline). These famous PV cells are utilized to validate the performance of the offered TDM. Table 1 depicts the behaviors of famous PV panels recorded under the STC. The primary purpose of these commercial PV panels is to validate the efficacy of the hybrid AV–GWO approach-based TDM compared to other approaches-based TDM.

7.1. Optimization results

The optimization outcomes are achieved by minimizing the fitness function ($\boldsymbol{\varepsilon}$) in (6) using the proposed hybrid AV–GWO approach and other optimization methods. Notably, the optimization process, simulation, and numerical data for all approaches are designed using MATLAB 2016*b* (Release, 2016b) and performed using a laptop running Windows 10 Enterprise 64-bit

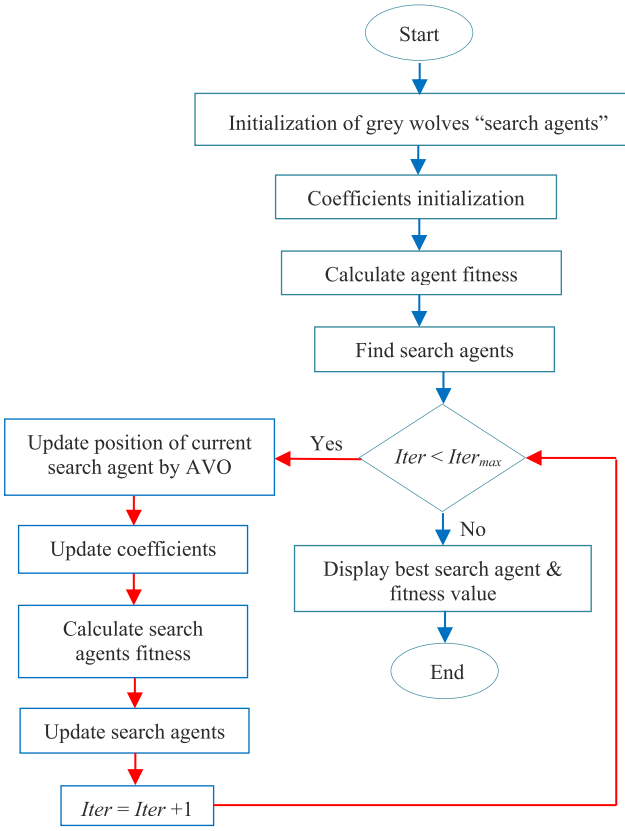

Fig. 5. Flowchart of the offered hybrid AV–GWO approach.

Table 1
Datasheet of two marketable PV panels.

Company	Kyocera (2018)	Solarex (2018)
Model	KC200GT	MSX-60
Cell Type	Multi-crystal	Polycrystalline
P_m [W]	200	60
V_m [V]	26.3	17.1
I_m [A]	7.61	3.5
V_{oc}[V]	32.9	21.1
I_{sc} [A]	8.21	3.8
N_s [cell]	54	36
K_i [A/°C]	0.00318	0.00065
K_V [V/°C]	−0.123	−0.08

Table 2
Characteristics of the hybrid AV–GWO approach.

No. of iterations	500
No. of search agents	30
No. of variables	9
L_1	0.7
L_2	0.3
w	3
P_1	0.6
P_2	0.4
P_3	0.6
No. of grey wolves	9

Table 3
Optimal nine parameters using AVO approach.

Parameter	KC200GT	MSX-60
I_{PV} [A]	8.2541	3.5712
R_p [Ω]	334.185	282.156
R_s [Ω]	0.3698	0.17194
a_1	1.3158	1.4162
a_2	1.1985	1.0126
a_3	1.5625	1.3185
I_{o1} [A]	2.745e−08	2.941e−08
I_{o2} [A]	4.925e−10	3.419e−10
I_{o3} [A]	4.573e−10	4.097e−10

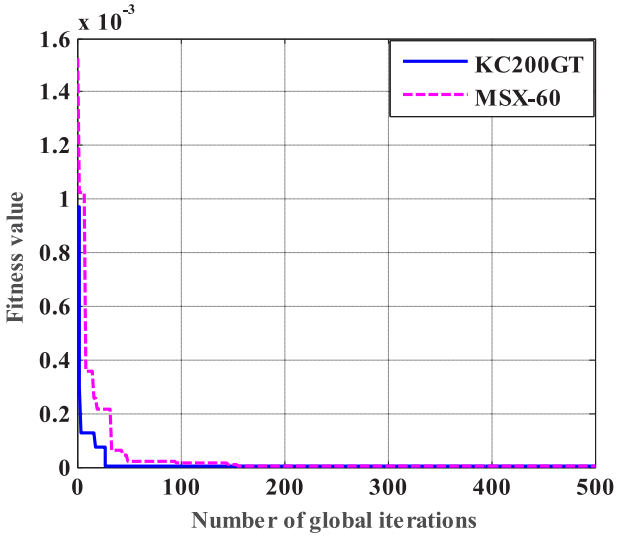

Fig. 6. Fitness function convergence for two marketable PV panels.

and outfitted with Inter(R) Core(TM) i7-4510 CPU @2.00 GHz 2.60 GHz processor and installed 16 GB RAM. The proper setting of the hybrid AV–GWO approach is depicted in Table 2. These settings are chosen based on the tradeoff between algorithm precision and intricacy. They are adjusted using the trial-and-error approach, a general method for adapting the algorithm parameters. In the optimization process, the hybrid AV–GWO was terminated after a high number of separate runs, around thirty runs of the offered approach for the practical PV modules. The provided hybrid AV–GWO has achieved the optimal solution faster than other approaches and attained the lowest fitness values that recorded 8.475e−13 and 7.412e−12 for KC200GT and MSX-60, respectively. Fig. 6 shows the best fitness value convergence curves using these marketable PV panels, indicating a very fast convergence speed. The optimal nine parameters of the TDM for both PV panels are mentioned in Table 3.

To confirm the soundness of the achieved designed variables, a fair comparison is done using the hybrid AV–GWO approach, the SOA, the simulated annealing (SA), WOA, GWO, and AVO for the two mentioned PV panels and indicated in Tables 4–5. Notably, for the two PV panels, the optimum parameters obtained using the hybrid AV–GWO are comparable to those obtained using other algorithms. They are within the allowable limit of PV modeling precision. As a result, the hybrid AV–GWO approach-TDM is a very competitive technology to those established PV models.

7.2. Computational and statistical analysis

Table 6 displays the calculation times for the meta-heuristic approaches utilized in this study, in which the hybrid AV–GWO takes the shortest time. Moreover, Tables 7–8 indicate the statistical analysis, such as average and standard deviation, to evaluate the optimal values for the two marketable PV panels using different optimization algorithms. Obviously, the novel hybrid AV–GWO has achieved the lowest standard deviation, median, and variance values compared to other approaches, which refers to the superior performance and good design of the novel hybrid AV–GWO approach.

Table 4
Comparison of optimal TDM parameters for KC200GT.

Parameter	SOA	SA	WOA	GWO	AVO	AV–GWO
I_{PV} [A]	8.21213	8.25	8.231	8.129	8.419	8.2541
R_p [Ω]	606.1219	327.597	341.387	351.264	361.821	334.185
R_s [Ω]	0.23796	0.378	0.3421	0.3491	0.3581	0.3698
a_1	1.2481	1.199	1.32	1.208	1.307	1.3158
a_2	1.991	1.2	1.236	1.172	1.137	1.1985
a_3	1.8421	1.48	1.0216	1.4272	1.5061	1.5625
I_{01} [A]	4.30e−08	1.78e−08	2.692e−08	2.578e−8	2.642e−08	2.745e−08
I_{02} [A]	2.22e−10	3.76e−10	4.678e−10	4.472e−10	4.814e−10	4.925e−10
I_{03} [A]	1.35e−6	4.62e−10	4.927e−10	4.973e−10	4.649e−10	4.573e−10
Fitness value	7.391e−11	8.469e−11	5.1497e−11	6.149e−11	7.249e−12	8.475e−13

Table 5
Comparison of optimal TDM parameters for MSX-60.

Parameter	SOA	SA	WOA	GWO	AVO	AV–GWO
I_{PV} [A]	3.80111	3.792	3.756	3.642	3.491	3.5712
R_p [Ω]	578.3468	298.59	277.37	280.41	281.974	282.156
R_s [Ω]	0.20598	0.211	0.195	0.1851	0.6972	0.17194
a_1	1.282	1.29	1.30	1.362	1.3901	1.4162
a_2	1.8043	1.22	1.23	1.1812	1.0841	1.0126
a_3	1.4364	1.28	1.13	1.174	1.3024	1.3185
I_{01} [A]	4.98e−8	1.98e−8	2.19e−8	2.842e−08	2.904e−08	2.941e−08
I_{02} [A]	7.24e−10	4.76e−10	3.68e−10	3.541e−10	3.414e−10	3.419e−10
I_{03} [A]	1.42e−7	2.62e−10	3.97e−10	4.017e−10	4.076e−10	4.097e−10
Fitness value	8.167e−11	3.149e−10	4.195e−11	6.149e−10	3.974e−11	7.412e−12

Table 6
Computing time of applied optimization methods in seconds.

PV cell	SOA	SA	WOA	GWO	AVO	AV–GWO
KC200GT	0.5621 (s)	0.5314 (s)	0.4836 (s)	0.4694 (s)	0.4410 (s)	0.4341 (s)
MSX-60	0.4621 (s)	0.4376 (s)	0.3697 (s)	0.3416 (s)	0.3301 (s)	0.3142 (s)

Table 7
Statistical analysis of fitness function for thirty separate runs for modeling of KC200GT.

Statistical analysis	SOA	SA	WOA	GWO	AVO	AV–GWO
Minimum	7.391e−11	8.469e−11	5.1497e−11	6.149e−11	7.249e−12	8.475e−13
Average	4.348e−10	4.927e−10	3.761e−10	3.173e−10	3.491e−11	4.268e−12
Standard	5.972e−10	6.491e−10	4.649e−10	4.975e−10	4.691e−11	5.475e−12

Table 8
Statistical analysis of fitness function for thirty separate runs for modeling of MSX-60.

Statistical analysis	SOA	SA	WOA	GWO	AVO	AV–GWO
Minimum	8.167e−11	3.149e−10	4.195e−11	6.149e−10	3.974e−11	7.412e−12
Average	4.192e−10	1.279e−9	2.178e−10	3.495e−9	1.373e−10	4.973e−11
Standard	6.184e−10	2.135e−9	3.197e−10	4.719e−9	2.349e−10	6.794e−11

7.3. Simulation outcomes under different environmental conditions

PV modules are susceptible to various environmental parameters, the most important of which are solar radiations and ambient temperature that affect the output current of PVs. The numerical results of the TDMs for the two commercial PV panels are compared with the measured data under various temperatures and solar irradiations to validate the efficacy of the AV-GWO-based TDM. The estimated TDM for the KC200GT PV panel is examined under different temperatures and constant G = 1000 W/m^2. Fig. 7(a)&(b) compares the *I-V* and *P-V* behaviors using the hybrid AV–GWO algorithm-based TDM with their experimental data for the KC200GT PV panel under several temperatures. It can be noted that the numerical results are matched with the experimental results using the hybrid AV-GWO-based TDM, which refers to the superiority of the offered approach for the PV panel. In addition, it is illustrated that the open circuit voltage and power fall as the temperature rises, whereas the short circuit current marginally rises. Moreover, the estimated TDM is examined under various irradiations and constant T = 25 °C for the KC200GT PV panel. Fig. 8(a)&(b) illustrates the *I-V* and *P-V* relationships of the hybrid AV-GWO-based TDM compared with their experimental data for the KC200GT PV module under various irradiations and constant T = 25 °C.

It is noted that there are no differences in the numerical and experimental results, which refers to the validity of the novel hybrid AV–GWO approach-TDM. Additionally, it is indicated that short circuit current drops when solar radiation falls, yet, open circuit voltage decreases somewhat as solar radiation lowers.

Fig. 9(a)&(b) indicates the *I-V* and *P-V* behaviors for the MSX-60 PV panel under various temperatures and constant G = 1000 W/m^2 using the AV–GWO algorithm-based TDM PV module. Notably, the numerical and measured results are close to this PV panel. So, the TDM can be utilized to determine the

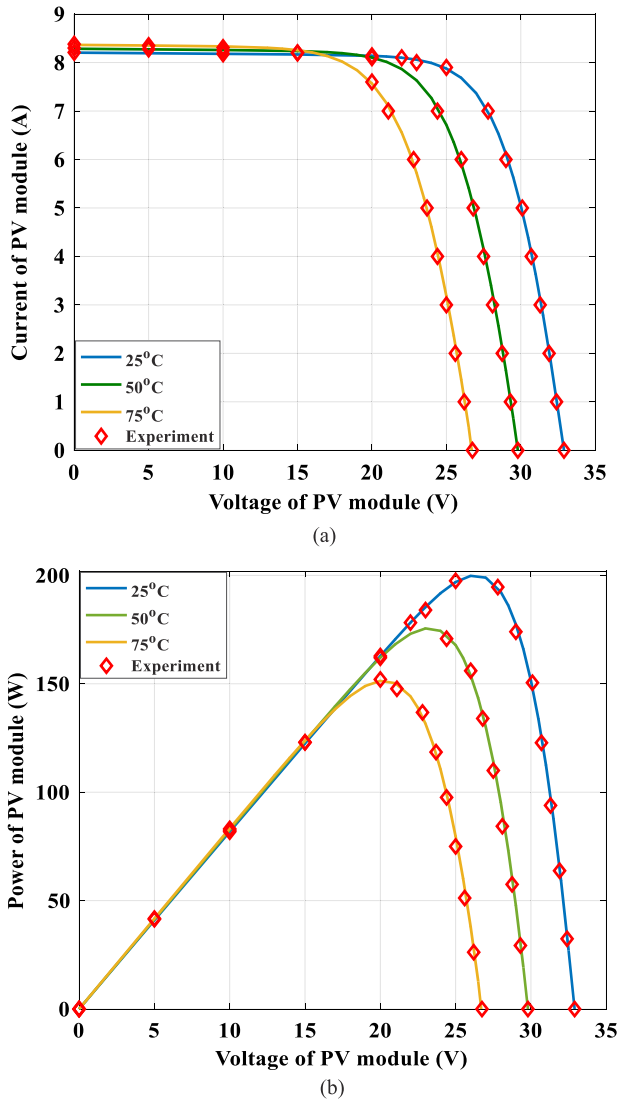

Fig. 7. Numerical outcomes and measured data of the KC200GT PV panel at several T, G = 1000 W/m^2. (a) *I-V* curves. (b) *P-V* curves.

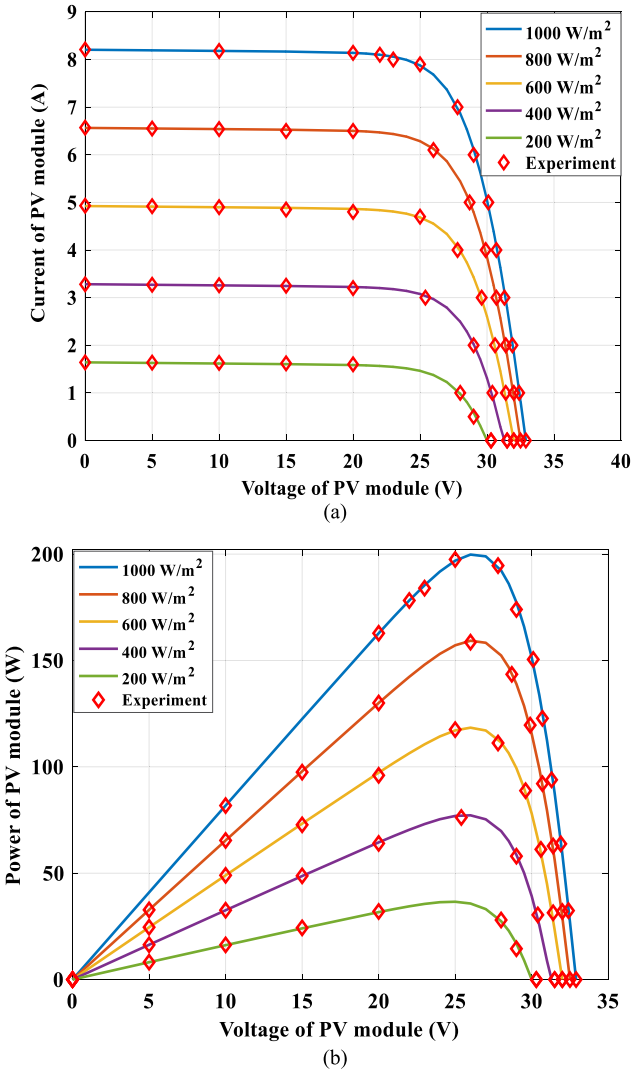

Fig. 8. Numerical outcomes and measured data of the KC200GT PV panel at various G and T = 25 °C. (a) *I-V* curves. (b) *P-V* curves.

electrical parameters of any PV panel and reasonably confirm the soundness of the AV–GWO approach.

Notably, all the measured values for actual PV panels are obtained on the outside surface of a Campus building roof. A real KC200GT PV panel (Kyocera, 2018) used in the experimental test is mentioned in Fig. 10(a). The PV panels are housed in an open-glassed container with flowing cold or hot to adjust the PV panels' ambient temperature, as depicted in Fig. 10(b). The experiment was carried out on 20 August 2021 at the Faculty of Engineering, Ain Shams University, Cairo, Egypt. The *I* & *V* values for both actual PV modules are measured with an ammeter and a voltmeter under various climatic circumstances. A variable resistor with a nominal value of 39 Ω is employed to record the *I* & *V* values at short-circuit, open-circuit, and varied load situations. The solar irradiation is measured using a silicon cell Pyranometer SP-110-SS with 5 W/m^2 per mV element of calibration and ±5% uncertainty in calibration. Moreover, a high probe infrared electronic thermometer temperature device with a setting of ±1 °C, whose range is [−32, 550 °C], is used to record the temperature.

For additional confirmation of the offered model, the ACE of the hybrid AV–GWO algorithm-based TDM related to the measured results is paralleled with other PV models, such as the WOA-based TDM (Elazab et al., 2018) and the iteration method-based TDM (Villalva et al., 2009) for the KC200GT and MSX-60 PV panels, which are indicated in Fig. 11(a)&(b). It can be noted here that the ACE of the hybrid AV-GWO-based TDM is significantly smaller than that of other PV models, which refers to the superiority of the proposed TDM, especially at the enclosure of all PV panel practical applications. The excellent efficiency and preciseness of the AV-GWO-based TDM refer to the suitable design of the hybrid AV–GWO approach.

8. Conclusion

A novel hybrid AV–GWO algorithm and a new fitness function to accurately identify the TDM PV parameters are proposed in this paper. The principle goal here is to achieve a precise model for any practical PV modules, which is critical in the simulation analyses of grid-integrated PV power plants. The PV cell is described by a nonlinear *I-V* characteristic, which includes nine parameters

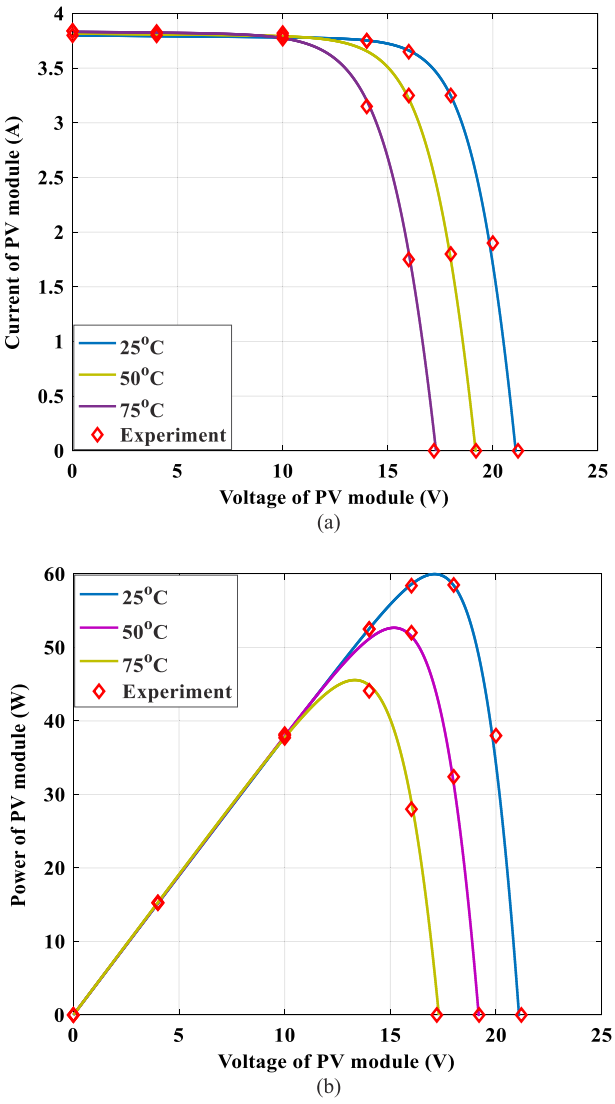

Fig. 9. Numerical and measured outcomes of the MSX-60 PV panel at various T, G = 1000 W/m^2. (a) *I-V* curves. (b) *P-V* curves.

due to the insufficiency of information supplied in the datasheet of such PV cells. In the optimization process, the hybrid AV–GWO minimizes the fitness function designed by the sum of the absolute current error, the squared current error, and the current error to the power of four. Hence, the nine TDM parameters of the PV panel can be extracted. Different comparisons were made to confirm the soundness of the proposed TDM using the hybrid AV–GWO technology. The AV–GWO approach was used to determine the parameters for two practical PV panels precisely. It is worth noting that the optimal nine parameters retrieved using the hybrid AV–GWO methodology are close to those obtained using other optimization methods. The AV–GWO has yielded lower optimum fitness values of 8.475e−13 and 7.412e−12 for KC200GT and MSX-60 PV panels. In addition, the AV–GWO has recorded the shortest computing time in 0.43412 (s) and 0.3142 (s) for KC200GT and MSX-60 PV panels, respectively. Moreover, the simulation evaluations of the hybrid AV-GWO-based TDM agree with the measured results under various environmental circumstances, and the error between these results is less than 0.4%. Furthermore, the hybrid AV–GWO approach has achieved a fast convergence speed and the best statistical optimization outcomes, which has proved the robustness of the AV–GWO in

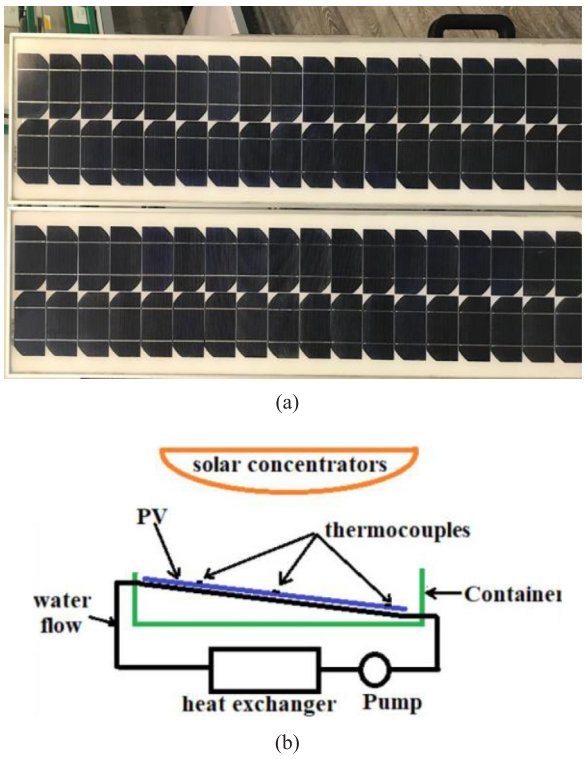

Fig. 10. Experimental set-up. (a) Practical KC200GT PV panel in the laboratory. (b) PV temperature regulation.

designing the optimum TDM parameters compared to the other approaches. For these actual PV modules, the ACE of the AV-GWO-based TDM related to the measured data has revealed a lower value over other PV models, which indicates the high performance of the offered approach in creating an accurate TDM-based PV module. The hybrid AV–GWO approach can realize the electrical parameters of any marketable PV panel.

For future work, the hybrid AV–GWO algorithm will be applied to design the controllers' parameters utilized in different energy conversion systems.

CRediT authorship contribution statement

Mahmoud A. Soliman: Methodology, Formal analysis, Writing – original draft. **Hany M. Hasanien:** Conceptualization, Methodology, Editing, Supervision. **Rania A. Turky:** Visualization, Investigation, Editing. **S.M. Muyeen:** Conceptualization, Methodology, Editing, Supervision.

Declaration of competing interest

The authors declare that they have no known competing financial interests or personal relationships that could have appeared to influence the work reported in this paper.

Data availability

The authors are unable or have chosen not to specify which data has been used.

Acknowledgment

The publication of this article was funded by Qatar National Library.

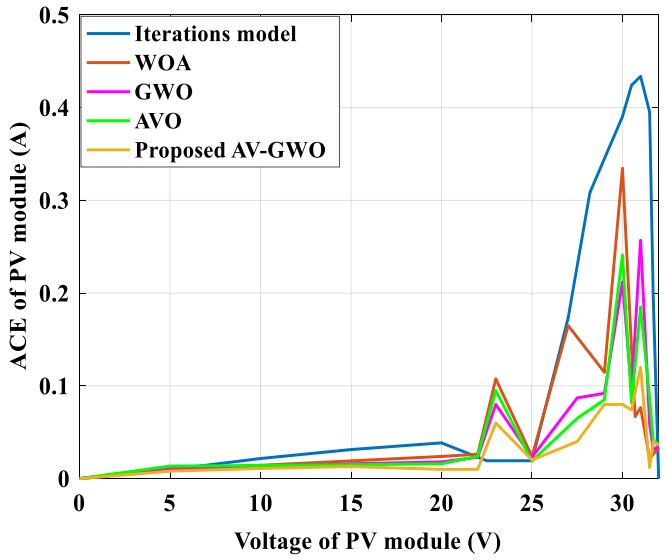

(a)

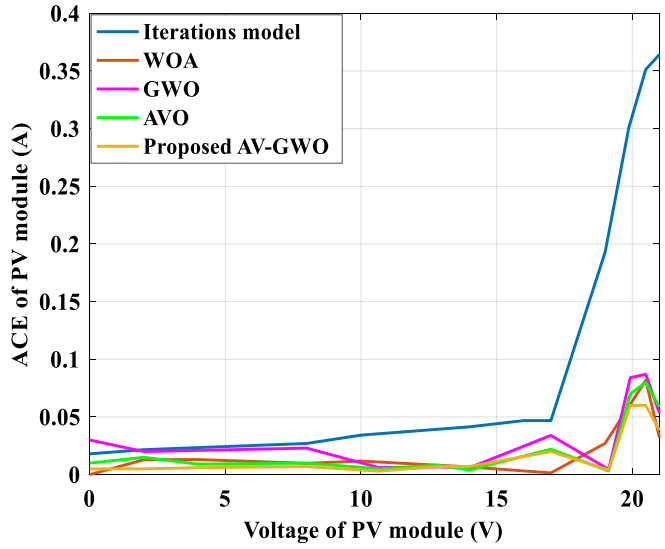

(b)

Fig. 11. ACE of PV panel. (a) KC200GT. (b) MSX-60.

References

Abdollahzadeh, Benyamin, Gharehchopogh, Farhad Soleimanian, Mirjalili, Seyedali, 2021. African vultures optimization algorithm: A new nature-inspired metaheuristic algorithm for global optimization problems. Comput. Ind. Eng. 158 (107408), 1–55.

Awadallah, Mohamed A., Venkatesh, Bala, 2016. Bacterial foraging algorithm guided by particle swarm optimization for parameter identification of photovoltaic modules. Canad. J. Electr. Compon. Eng. 39 (2), 150–157.

Bastidas-Rodriguez, J.D., Petrone, G., Ramos-Paja, C.A., Spagnuolo, G., 2017. A genetic algorithm for identifying the single diode model parameters of a photovoltaic panel. Math. Comput. Simul. 131, 38–54.

Bradaschia, Fabricio, Cavalcanti, Marcelo C., do Nascimento, Aguinaldo José, da Silva, Emerson Alves, et al., 2019a. Parameter identification for PV modules based on an environment-dependent double-diode model. IEEE J. Photovolt. 9 (5), 1388–1397.

Bradaschia, Fabricio, Cavalcanti, Marcelo C., do Nascimento, Aguinaldo José, et al., 2019b. Parameter identification for PV modules based on an environment-dependent double-diode model. IEEE J. Photovolt. 9 (5), 1388–1397.

Chatterjee, A., Keyhani, A., Kapoor, D., 2011. Identification of photovoltaic source models. IEEE Trans. Energy Convers. 26 (3), 883–889.

Chennoufi, Khalid, Ferfra, Mohammed, Mokhlis, Mohcine, 2021. An accurate modelling of photovoltaic modules based on two-diode model. Sol. Energy 167, 294–305.

De Soto, W., Klein, S., Beckman, W., 2006. Improvement and validation of a model for photovoltaic array performance. Sol. Energy 80 (1), 78–88.

Di Piazza, M.C., Luna, M., Petrone, G., Spagnuolo, G., 2017. Translation of the single-diode PV model parameters identified by using explicit formulas. IEEE J. Photovolt. 7 (4), 1009–1016.

Diab, Ahmed A. Zaki, Sultan, Hamdy M., Aljendy, Raseel, Al-Sumaiti, Ameena Saad, Shoyama, Masahito, Ali, Ziad M., 2020. Tree growth based optimization algorithm for parameter extraction of different models of photovoltaic cells and modules. IEEE Access 8, 2169–3536.

El-Fergany, Attia A., 2021. Parameters identification of PV model using improved slime mould optimizer and Lambert W-function. Energy Rep. 7, 875–887.

El-Fergany, Attia A., Hasanien, Hany M., 2015. Single and multi-objective optimal power flow using grey wolf optimizer and differential evolution algorithms. Electr. Power Compon. Syst. 43 (13), 1548–1559.

Elazab, Omnia S., Hasanien, Hany M., Elgendy, Mohamed A., Abdeen, Amr M., 2018. Parameters estimation of single- and multiple-diode photovoltaic model using whale optimisation algorithm. IET Renew. Power Gener. 12 (15), 1755–1761.

Gao, Xiankun, Cui, Yan, Hu, Jianjun, Xu, Guangyin, et al., 2018. Parameter extraction of solar cell models using improved shuffled complex evolution algorithm. Energy Convers. Manage. 157, 460–479.

Houssein, Essam H., Zaki, Gamela Nageh, Diab, Ahmed A. Zaki, Younis, Eman M.G., 2021. An efficient manta ray foraging optimization algorithm for parameter extraction of three-diode photovoltaic model. Comput. Electr. Eng. 94, 1–22.

Ibrahim, I.A., Hossain, M.J., Duck, B.C., Nadarajah, M., 2020. An improved wind driven optimization algorithm for parameters identification of a triple-diode photovoltaic cell model. Energy Convers. Manage. 213 (112872).

JackChin, Vun, Salam, Zainal, 2019. Coyote optimization algorithm for the parameter extraction of photovoltaic cells. Sol. Energy 194, 656–670.

Kassis, A., Saad, M., 2010. Analysis of multi-crystalline silicon solar cells at low illumination levels using a modified two-diode model. Sol. Energy Mater. Sol. Cells 94 (12), 2108–2112.

Khanna, V., Das, B.K., Singh, P.K., Panwar, Vandana, 2015. A three diode model for industrial solar cells and estimation of solar cell parameters using PSO algorithm. Renew. Energy 78, 105–113.

Kyocera, 2018. KC200gt kyocera PV module datasheet. [Online]. Available: http://www.kyocera.com.sg/products/solar/pdf/kc200gt.pdf. [Accessed: 01-Dec-2018].

Li, Shuijia, Gong, Wenyin, Wang, Ling, Yan, Xuesong, Hu, Chengyu, 2020. A hybrid adaptive teaching–learning-based optimization and differential evolution for parameter identification of photovoltaic models. Energy Convers. Manage. 225 (113474), 1–15.

Li, Shuijia, Gong, Wenyin, Yan, Xuesong, Hu, Chengyu, Bai, Danyu, Wang, Ling, Gao, Liang, 2019. Parameter extraction of photovoltaic models using an improved teaching-learning-based optimization. Energy Convers. Manage. 237, 293–305.

Ma, Tao, et al., 2021. Performance modelling of photovoltaic modules under actual operating conditions considering loss mechanism and energy distribution. Appl. Energy 298.

Marques Gomes, Ruan Carlos, Vitorino, Montiê Alves, Rossiter Corrêa, Maurício Beltrão de, Fernandes, Darlan Alexandria, 2017. Shuffled complex evolution on photovoltaic parameter extraction: A comparative analysis. IEEE Trans. Sustain. Energy 8 (2), 805–815.

Mirjalili, S., Mirjalili, S.M., Lewis, A., 2014. Grey wolf optimizer. Adv. Eng. Softw. 69 (3), 46–61.

Oliva, D., Aziz, M.A.E., Hassanien, A.E., 2017. Parameter estimation of photovoltaic cells using an improved chaotic whale optimization algorithm. Appl. Energy 200, 141–154.

Oliva, Diego, Cuevas, Erik, Pajares, Gonzalo, 2014. Parameter identification of solar cells using artificial bee colony optimization. Sol. Energy 72, 93–102.

Patro, Sanat Kumar, Saini, R.P., 2020. Mathematical modeling framework of a PV model using novel differential evolution algorithm. Sol. Energy 211, 210–226.

Polo, Jesús, Martín-Chivelet, Nuria, Carmen Alonso-García, M., Zitouni, Houssain, Alonso-Abella, Miguel, Sanz-Saiz, Carlos, Vela-Barrionuevo, Nieves, 2019. Modeling I-V curves of photovoltaic modules at indoor and outdoor conditions by using the Lambert function. Energy Convers. Manage. 195, 1004–1011.

PV Power Plants, 2020. Global industry guide [online]. Available: http://www.renewableenergyworld.com.

Qais, Mohammed H., Hasanien, Hany M., Alghuwainem, Saad, 2019. Identification of electrical parameters for three-diode photovoltaic model using analytical and sunflower optimization algorithm. Appl. Energy 250, 109–117.

Ramadan, Abdelhady, Kamel, Salah, Hussein, Mahmoud M., Hassan, Mohamed H., 2021. A new application of chaos game optimization algorithm for parameters extraction of three diode photovoltaic model. IEEE Access 9, 51582–51594.

Release, 2016b. 2016b, "*MATLAB*". The Math Works Press, Sep., [accessed 13 Sept., 2017].
Rezk, H., Babu, T.S., Dhaifallah, M.A., Ziedan, H.A., 2021. A robust parameter estimation approach based on stochastic fractal search optimization algorithm applied to solar PV parameters. Energy Rep. 7, 620–640.
Ridha, Hussein Mohammed, Heidari, Ali Asghar, Wang, Mingjing, Chen, Huiling, 2020. Boosted mutation-based harris hawks optimizer for parameters identification of single-diode solar cell models. Energy Convers. Manage. 209 (112660), 1–14.
Ridha, Hussein Mohammed, Hizam, Hashim, Gomes, Chandima, et al., 2021. Parameters extraction of three diode photovoltaic models using boosted LSHADE algorithm and Newton Raphson method. Energy 224 (120136), 1–18.
Rizk-Allah, R.M., El-Fergany, A.A., 2021. Emended heap-based optimizer for characterizing performance of industrial solar generating units using triple diode model. Energy 237 (121561).
Şenturk, A., 2018. New method for computing single diode model parameters of photovoltaic modules. Renew. Energy 128, 30–36.
Sera, D., Teodorescu, R., Rodriguez, P., 2007. PV panel model based on datasheet values. In: Proc. IEEE Int. Symp. Ind. Electron. Vigo, Spain. pp. 2392–2396.
Sharma, Abhishek, Sharma, Abhinav, Dasgotra, Ankit, Jately, Vibhu, Ram, Mangey, Rajput, Shailendra, Averbukh, Moshe, Azzopardi, Brian, 2021a. Opposition-based tunicate swarm algorithm for parameter optimization of solar cells. IEEE Access 9, 125590–125602.
Sharma, Abhishek, Sharma, Abhinav, Dasgotra, Ankit, Jately, Vibhu, Ram, Mangey, et al., 2021b. Opposition-based tunicate swarm algorithm for parameter optimization of solar cells. IEEE Access 9, 125590–125602.
Solarex, 2018. MSX-60 PV module solarex datasheet. [Online]. Available: http://www.solarelectricsupply.com/solarpanels/solarex/solarex-msx-60-w-junctionbox. [Accessed: 01-Dec-2018].
Soliman, M.A., et al., 2018. Hybrid ANFIS-GA-based control scheme for performance enhancement of a grid-connected wind generator. IET Renew. Power Gener. 12 (7), 832–843.
Toledo, F.J., Blanes, J.M., Galiano, V., 2018. Two-step linear least-squares method for photovoltaic single-diode model parameters extraction. IEEE Trans. Ind. Electron. 65 (8), 6301–6308.
Villalva, M.G., Gazoli, J.R., Filho, E.R., 2009. Comprehensive approach to modeling and simulation of photovoltaic array. IEEE Trans. Power Electron. 24 (5), 1198–1208.
Weng, X., et al., 2021. Laplacian nelder–mead spherical evolution for parameter estimation of photovoltaic models. Energy Convers Manag. 243 (114223).
Yousri, Dalia, Fathy, Ahmed, Rezk, Hegazy, Thanikanti, Sudhakar Babu, Berber, Mohamed R., 2021. A reliable approach for modeling the photovoltaic system under partial shading conditions using three diode model and hybrid marine predators-slime mould algorithm. Energy Convers. Manage. 243 (114269), 1–17.
Yousri, D., Rezk, H., Fathy, A., 2020a. Identifying the parameters of different configurations of photovoltaic models based on recent artificial ecosystem-based optimization approach. Int. J. Energy Res. 44, 11302–11322.
Yousri, Dalia, Thanikanti, Sudhakar Babu, Allam, Dalia, Ramachandaramurthy, Vigna K., Eteiba, M.B., 2020b. Fractional chaotic ensemble particle swarm optimizer for identifying the single, double, and three diode photovoltaic models' parameters. Energy 195, 1–15.
Zhang, Hongliang, Heidari, Ali Asghar, Wang, Mingjing, Zhan, Lejun, Chen, Huiling, Li, Chengye, 2020a. Orthogonal nelder–mead moth flame method for parameters identification of photovoltaic modules. Energy Convers. Manage. 211 (112764), 1–24.
Zhang, Yiying, Jin, Zhigang, Mirjalili, Seyedali, 2020b. Generalized normal distribution optimization and its applications in parameter extraction of photovoltaic models. Energy Convers. Manage. 211 (113301), 1–14.
Zhou, W., Wang, P., Heidari, A.A., X. Zhao, X., et al., 2021. Random learning gradient based optimization for efficient design of photovoltaic models. Energy Convers. Manage. 230.